

The Static and Dynamic Behavior of Reinforced Concrete Beams with Cracking Due to Alkali-Silica Reaction

Manabu Fujii

*Department of Civil Engineering
Kobe University
Kobe, Japan*

Takayuki Kojima

*Department of Civil Engineering
Ritsumeikan University
Kyoto, Japan*

Kazuo Kobayashi

*Department of Civil Engineering
Kyoto University
Kyoto, Japan*

Hiroshi Maehara

*Hanshin Expressway Public Corporation
Osaka, Japan*

ABSTRACT

T-shaped piers of the Hanshin Expressway in Osaka have deteriorated as a result of alkali-silica reaction(ASR). It was decided that some model tests should be carried out to evaluate the safety of existing deteriorated structures (Blight 1983), (Poitevin 1983).

In this study, a total of 26 model reinforced concrete beams were fabricated by using the same aggregate as that in the deteriorated structure. The effect of steel ratio and arrangement of steel bars on expansion and deterioration due to ASR, and the static and dynamic behaviors of the deteriorated beams were investigated.

1. OUTLINE OF THE TESTS

The test program was divided into two parts. In Part I the effect of steel ratio and arrangement of steel bars on deterioration was examined, and the specimens after the expansion due to ASR reached the given value were tested under static loading. The specimen had a dimension of 15x15x170cm. The steel ratios and arrangement of steel bars are listed in **Table 1**. Concrete mixes N1 and A1 as listed in **Table 2** were used in Part I as normal and ASR concrete respectively. Crushed gravel(Bronzite Andesite) produced in Teshima Island was used as the reactive coarse aggregate. In order to accelerate the reaction, surplus alkali(NaOH) was added in each mix, and the specimens of ASR concrete were cured under the accelerated condition of 40°C and R.H.100% after curing for two weeks at 20°C. The expansion of the ASR specimens was measured by electric strain gauges attached to the longitudinal bars and the stirrups. In the static loading test, symmetrical two point loading was adopted as illustrated in **Fig.1**, in which the shear span effective depth ratio (a/d) was chosen to be 2.5. The load was applied to the specimen monotonically up to its design value defined in such a way that the calculated steel stress became 1800kgf/cm^2 , and was unloaded and then reloaded up to failure. At each load increment, mid span deflection and steel stresses were measured.

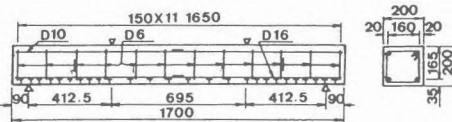
In Part II static and fatigue behaviors of reinforced concrete beams which had the same dimension as that in Part I were investigated. The steel

Table 1 Details of Specimens and Test Results

Part	Beam	mix	tension steel As pl (%)	compression steel As' pl' (%)	stirrups pv (cm)	ultimate load test (t)	ultimate load cal. (t)	design load (t)	type of failure
I	I1A	A1	2016 1.20	2010 0.43	10 0.3	14.50	10.66	4.85	F
	I2N	N1	2016 1.20	2010 0.43	15 0.2	13.65	11.04	4.85	S
	I2A	A1	2016 1.20	2010 0.43	15 0.2	14.65	10.66	4.85	F
	I3N	N1	2019 1.74	2010 0.43	10 0.3	20.00	18.87	6.87	F
	I3A	A1	2019 1.74	2010 0.43	10 0.3	19.05	15.12	6.87	F
	I4N	N1	2019 1.74	2010 0.43	15 0.2	20.15	18.87	6.87	S
	I4A	A1	2019 1.74	2010 0.43	15 0.2	18.30	15.12	6.87	F
	I5N	N1	2013 0.77	2013 0.77	10 0.3	6.25	5.55	3.16	F
I5A	A1	2013 0.77	2013 0.77	10 0.3	6.00	5.19	3.16	F	
II	I6N	N1	2016 1.20	2016 1.20	10 0.3	13.75	11.04	4.83	F
	I6A	A1	2016 1.20	2016 1.20	10 0.3	13.50	10.53	4.83	F
	I10N	N2				13.75	10.08	4.85	F
	I10A	A2	2016 1.20	2010 0.43	15 0.2	13.75	9.85	4.85	F
	I18N	N2				13.30	9.83	4.85	F
	I18A	A2				13.15	10.07	4.85	F
	I19N	N3				12.50	9.63	4.85	F

note: In the calculation of ultimate load, measured values of concrete strength (Table 3) and yield strength of steel were used.

F: flexural failure due to yielding of steel bar, S: shear failure


Fig.1 Specimen and Arrangement of Reinforcing Bars

ratio and arrangement of steel bars were the same as Beam I2 in Part I. Four levels of deterioration were chosen so that measured stirrup strain became about 500, 1000, 1500x10⁻⁶ and the maximum value for C, B, A and SA series respectively. Concrete mixes N2, A2 and A3 in **Table 2** were used. Mixes N2 and A2 were almost the same as N1 and A1 respectively, but NaCl was used as additional alkali in Part II, and the sampling time of the reactive aggregate was different. In mix A3 nearly the pessimum content of the reactive aggregate and more additional alkali were used to attain the most deteriorated level. The specimens which attained the given level of deterioration by accelerating curing were tested under static and dynamic loadings. The span and a/d ratio were the same as those in Part I. In the static test, five repetitions of loading from zero to the maximum load, in each step, were applied to the specimen. Five steps were set so that the maximum load in each step was varied at an equal increment from the design load (4.85t) to calculated ultimate load for Beam IIC(9.85t). In the fatigue test the minimum load was 1t and the maximum load was determined by the same manner as that in the static test. In each step 10⁵ repetitions of loading were applied to the specimen. When the specimen did not fail in the final step, the test was followed by an additional step at a higher maximum load increased by 1t. Deflection of the beam and strains of longitudinal bars and stirrups were measured in both tests.

Table 2 Details of Concrete Mixes

Part	series	mix	coarse aggregate	total eq.alkali	additional alkali
I	N	A1	normal* reactive**	6.0kg/m ³ 6.0	NaOH NaOH
		N	normal	6.0	NaCl
II	C, B, A, SA	N2	normal	6.0	NaCl
		A2	reactive ***	6.0	NaCl
		A3	***	8.0	NaCl

note: in all mixes, W/C=50%, S/a=44%, W=176kg/m³, max. size of aggregate; 20m

* :Iakatsuki crushed gravel
 ** :Ieshima crushed gravel(Bronzite Andesite)
 ***:mixture of normal and reactive aggregates (the mixture ratio=1:1)

2. TEST RESULTS AND DISCUSSIONS

Fig.2 shows, as an example, the strains measured at the middle of the longitudinal bars and the stirrup after the age of 14 days. Cracks due to

Table 3 Properties of Concrete
unit:kgf/cm²

Part	series	mix	compressive strength	tensile strength	Young's modulus(x10 ⁴)
I		M1	406(100)	28.1(100)	29.9(100)
		A1	241(59)	14.2(51)	10.1(33)
II	N	N2	503(100)	40.0(100)	33.7(100)
	C	A2	418(83)	26.8(67)	28.1(83)
	B	A2	422(84)	24.9(62)	29.8(88)
	A	A2	500(99)	26.8(67)	24.2(72)
	SA	A3	352(70)	19.4(49)	12.8(38)

() : ratio of ASR concrete to normal concrete(%)

ASR were observed about two weeks after accelerating curing, when the measured strain of the longitudinal bar reached about 200×10^{-6} . The cracks due to ASR occurred first along the longitudinal bars, and then also along the stirrups. Thereafter new cracks in another directions developed from the above cracks. After 50 days of accelerating curing, the rate of expansion decreased gradually, and the expansion became approximately constant at 100 days. Longitudinal strains were significantly affected by degree of constraint (steel ratio p_l), being $1532-1648 \times 10^{-6}$ for $p_l=0.43\%$, $1053-1279 \times 10^{-6}$ for $p_l=0.77\%$, $715-975 \times 10^{-6}$ for $p_l=1.20\%$ and $638-651 \times 10^{-6}$ for $p_l=1.74\%$ at the age of 153 days irrespective of compression and tension steel. Similar inclination was observed in lateral strain which was $1744-1859 \times 10^{-6}$ for $p_v=0.2\%$ and $1120-1540 \times 10^{-6}$ for $p_v=0.3\%$.

Concrete properties for the beam test are listed in **Table 3**. In Part I, compressive and tensile strengths and Young's modulus of A1 concrete were approximately 60%, 50% and 30% of normal concrete respectively. In Part II, the reduction of concrete properties depended on the levels of expansion, and the level of deterioration of A3 concrete was considered to be similar to that of A1 concrete in Part I.

The compressive stress introduced to the specimen (chemical prestress) of Part I by constraint of expansion due to ASR was approximately 40 kgf/cm^2 for all the specimens, and it was scarcely affected by arrangement and steel ratio of reinforcing bars. In Part II the prestress at the bottom fibers was 11, 17, 26 and 52 kgf/cm^2 for C, B, A and SA series respectively.

The reduction in load bearing capacity of the members deteriorated by ASR was expected especially for shear in the members with a lower web steel ratio when the test was programmed (Wood 1983), and then web steel ratio p_v was chosen to be 0.2% (minimum requirement for shear) and 0.3%. The ultimate load bearing capacity of the ASR specimen obtained from the experiment, however, was almost the same as, or slightly less than that of the specimen of normal concrete. The failure of the ASR specimen was determined by yielding of main reinforcing bar and crushing of concrete both in Part I and II, while shear failure occurred in two normal specimens I2N and I4N in Part I.

The crack pattern of the specimen after static loading test is shown in **Fig.3**. In ASR specimens there were not as many cracks due to loading in flexural span as in the normal concrete specimens. Then in shear span significant diagonal cracks such as are found were not observed in the ASR specimens, probably because the prestress due to the ASR expansion enhanced the shear strength more than the reduction of shear strength due to deterioration.

Fig.4 shows the relationships between load and mid span deflection. The reduction of Young's modulus and tensile strength of the ASR concrete cylinders as listed in **Table 3** suggests to decrease the rigidity at the

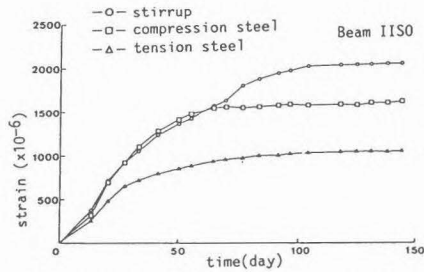


Fig.2 Relationship between Strains of Reinforcing Bars and Time

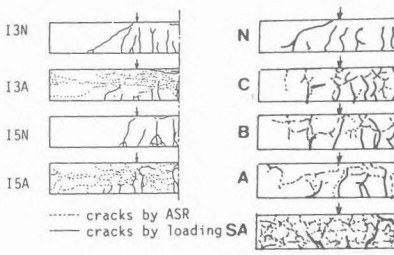


Fig.3 Crack Pattern after Static Test

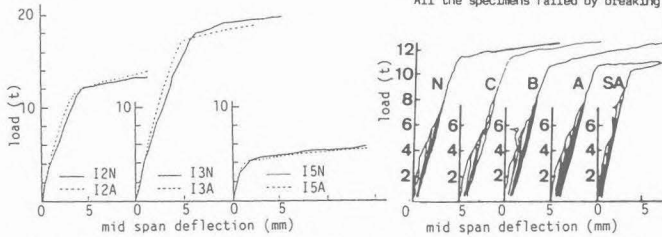


Fig.4 Relationship between Load and Mid Span Deflection

whole loading stage and the cracking strength of the beams. On the other hand the chemical prestress introduced by ASR expansion increased the cracking strength, and in addition the properties of the core concrete subjected to three dimensional constraint should be less deteriorated than those in Table 3 which were obtained with unconstrained specimens. The deflection of the ASR specimen in Part I was similar to that of each corresponding normal concrete specimen at a load stage prior to cracking, and the former was rather small than the latter after cracking as shown in Fig.4. The same inclination was observed in series SA of Part II, but the deflection of series A, B and C specimen was slightly greater than that of IINO one.

The relationships between load and stirrup strain obtained in Part II are shown in Fig.5. Since marked diagonal cracks did not occur in the ASR specimens because of the chemical prestress, the stirrup strain of the ASR specimen was remarkably less than that of IINO specimen.

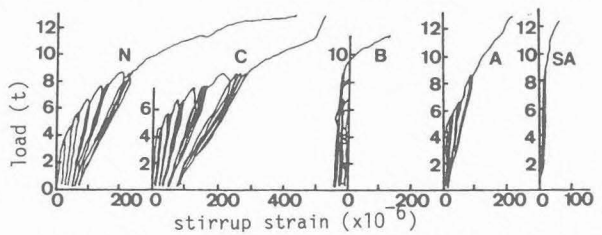


Fig.5 Relationship between Load and Stirrup Strain

The results of the fatigue test are listed in Table 4. The crack width, the mid span deflection, the strains of longitudinal bars and stirrups are shown in Figs. 6, 7, 8 and 9 respectively. In all the series the specimen failed by breaking of main steel due to fatigue. The crack patterns after fatigue test were similar to those after the static test. The crack width did not increase remarkably with repetition of loading except IIC1 specimen. The deflection as well as the crack width of IIC1 specimen

Table 4 Results of Fatigue Test

series	beam	max.load (t)	no.of cycles to failure*	failure occurred at
N	IIN1	10.85	28500	M
	IIN2	10.85	17400	S
C	IIC1	10.85	49800	M
	IIC2	10.85	72000	M
B	IIB1	11.85	5000	M
	IIB2	10.85	100000	M
A	IIA1	10.85	26800	M
	IIA2	10.85	41700	M
SA	IIS1	9.85	85000	M
	IIS2	9.85	58600	M

*:number of cycles in the step of the maximum load at which the specimen failed. The specimen had been already subjected to 100000 cycles of loading in each step.

M:flexural span, S:shear span
All the specimens failed by breaking of steel bar.

increased suddenly in the second step, but there was no significant difference in fatigue life. The number of cycles to failure of the ASR specimen was greater than that of the normal concrete specimen probably because the stress range of steel bar decreased by the chemical prestress as shown in Fig.8. The stirrup strain of the ASR specimen decreased with the level of expansion. As the result, deterioration due to ASR was not directly related to the reduction of fatigue properties of the specimen, but in some of the ASR specimen compressive strain increased with load repetitions.

3. CONCLUSIONS

The following conclusions may be drawn.

- (1) A decrease of the static load bearing capacity due to alkali-silica reaction was not observed.
- (2) Compressive stresses of 20-40kgf/cm² were introduced to the concrete of the ASR specimen by constraint of expansion due to reinforcement.
- (3) The diagonal cracks observed in the normal concrete specimen could not be clearly observed in the ASR specimen.
- (4) Deformational behavior of the ASR specimen was almost the same as that of the normal concrete specimen, although marked potential surface cracks due to the reaction were observed.
- (5) Fatigue failure was caused by breaking of main reinforcing bars in all the specimen, and the fatigue life was not affected by ASR.
- (6) Slight increase of bending compressive strain in some of the ASR specimen with increase of load repetitions was observed.

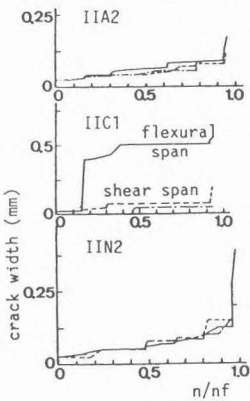


Fig.6 Crack Width

nf: number of cycles to failure

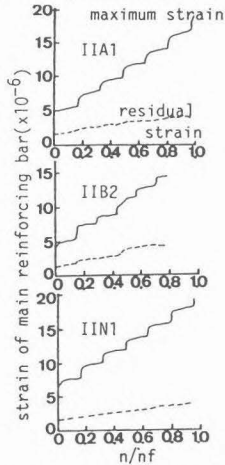


Fig.8 Strain of Main Reinforcing Bar

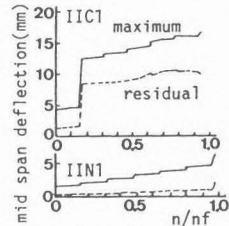


Fig.7 Mid Span Deflection

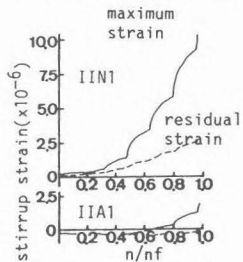


Fig.9 Strain of Stirrup

REFERENCES

- 1) Blight, C.E. and Alexander, M.G. 1983. In 6th International Conference on Alkalis in Concrete. ed. G.M.Idorn, pp401-410, Copenhagen.
- 2) Poitevin, P. 1983. In 6th International Conference on Alkalis in Concrete. ed. G.M.Idorn, pp391-399. Copenhagen.
- 3) Wood, J.G.M. and Wickens, P.J. 1983. In 6th International Conference on Alkalis in Concrete. ed. G.M.Idorn, pp487-494. Copenhagen.